Restorative Neurology and Neuroscience xx (20xx) x–xx
DOI 10.3233/RNN-170808
IOS Press

Phenelzine, a small organic compound mimicking the functions of cell adhesion molecule L1, promotes functional recovery after mouse spinal cord injury

Rong Li[a,1], Sudhanshu Sahu[a,1] and Melitta Schachner[a,b,*]
[a]*Center for Neuroscience, Shantou University Medical College, Shantou, Guangdong, China*
[b]*Keck Center for Collaborative Neuroscience and Department of Cell Biology and Neuroscience, Rutgers University, Piscataway, NJ, USA*

Abstract.
Background: Neural cell adhesion molecule L1 contributes to nervous system development and maintenance by promoting neuronal survival, neuritogenesis, axonal regrowth/sprouting, myelination, and synapse formation and plasticity. L1 also enhances recovery after spinal cord injury and ameliorates neurodegenerative processes in experimental rodent models. Aiming for clinical translation of L1 into therapy we screened for and functionally characterized *in vitro* the small organic molecule phenelzine, which mimics characteristic L1 functions.
Objective: The present study was designed to evaluate the potential of this compound *in vivo* in a mouse model of spinal cord injury.
Methods and Results: In mice, intraperitoneal injection of phenelzine immediately after severe thoracic compression, and thereafter once daily for 6 weeks, improved hind limb function, reduced astrogliosis and promoted axonal regrowth/sprouting at 4 and 5 weeks after spinal cord injury compared to vehicle control-treated mice. Phenelzine application upregulated L1 expression in the spinal cord and stimulated the cognate L1-mediated intracellular signaling cascades in the injured spinal cord tissue. Phenelzine-treated mice showed decreased levels of pro-inflammatory cytokines, such as interleukin-1β, interleukin-6, and tumor necrosis factor-α in the injured spinal cord during the acute phase of inflammation.
Conclusions: This study provides new insights into the role of phenelzine in L1-mediated neural functions and modulation of inflammation. The combined results raise hopes that phenelzine may develop into a therapeutic agent for nervous system injuries.

Keywords: L1, phenelzine, mouse, spinal cord injury, inflammation, regeneration

1. Introduction

Unlike fish and many non-mammalian vertebrates, the mammalian central nervous system has a very limited capacity for regeneration after acute or chronic injury, which leads to persistent functional deficits (Fehlings, 2008; Fitch & Silver, 2008). Several cellular and molecular mechanisms may underlie this limitation, including paucity of conducive, and

[1]These authors contributed equally

*Corresponding author: Melitta Schachner, Center for Neuroscience, Shantou University Medical College, 22 Xin Ling Road, Shantou, Guangdong 515041, China. Tel.: +86 754 8890 0276; Fax: +86 754 8890 0236; Email: schachner@stu.edu.cn and schachner@dls.rutgers.edu.

abundance of inhibitory contributions to the damaged tissue preventing to heal and to renew functions operant before injury (Giger et al., 2010). Among the recovery pro-active molecules is the neural cell adhesion molecule L1, which has been shown to promote not only axonal regrowth, guidance and fasciculation, but also to enhance neuronal survival, remyelination and synaptic plasticity in an inhibitory environment (Barbin et al., 2004; Lavdas et al., 2011; Irintchev & Schachner, 2012; Sytnyk et al., 2017). Since viral delivery of L1, application of recombinant L1, and injection of stem cells overexpressing L1 could meet difficulties in translation to therapy in humans, we have screened a library of small organic molecules - some of them FDA approved – for compounds that structurally and functionally mimic L1 and found phenelzine (PS) as a L1-mimetic small organic compound (Kataria et al., 2016).

PS belongs to the hydrazine class of organic compounds and is a non-selective, irreversible inhibitor of monoamine oxidase (MAO) that causes long-lasting increases in the levels of biogenic amines and is commonly used in the treatment of major depression, panic disorder and social anxiety disorder (Johnson et al., 1995; Parent et al., 2002). PS and its active metabolite β-phenylethylidene hydrazine are potent inhibitors of gamma-aminobutyric acid (GABA) transaminase, leading to surges in GABA levels in the central nervous system (Paslawski et al., 2001). PS has also been reported to be neuroprotective in animal models of ischemia-reperfusion brain injury and traumatic brain injury (Singh et al., 2013; Cebak et al., 2017).

Several studies in mammals have indicated that injury-induced glial cell activation and inflammation play important roles in preventing recovery after injury (Fitch & Silver, 2008; Huang et al., 2013; Levesque et al., 2013; Yoo et al., 2013). The biogenic amines serotonin (5-HT), norepinephrine (NE), dopamine (DA) and GABA all exhibit anti-inflammatory activities by modulating T-cell activation and cytokine release in several disease paradigms (Hofstetter et al., 2005; Yin et al., 2006; Levite, 2008; Bhat et al., 2010; Simonini et al., 2010). PS likely affects immune cell function by inhibiting MAO-A, which becomes up-regulated on the mitochondrial membrane of lymphocytes in response to inflammation (Chaitidis et al., 2004). Thus, MAO inhibition and sustained high concentrations of 5-HT, NE, DA and GABA, in response to PS, could modulate the inflammatory process at the lesion site following SCI. Despite these insights into the functions of PS, many cellular and molecular consequences underlying recovery have remained to be elucidated.

In the current study, we evaluated the effects of PS on the functional, biochemical and histological outcomes after SCI in mice. We found that PS treatment improves locomotor recovery following SCI, promotes axonal regrowth/sprouting, enhances remyelination, upregulates the expression of L1 and induces L1-medited intracellular signaling cascades in the injured spinal cord. We also demonstrate that daily PS treatment after SCI reduces inflammation and glial scar formation. These observations encourage the expectation that, in a mammalian clinically relevant paradigm, PS treatment can significantly reduce disease severity and improve motor functional outcomes.

2. Materials and methods

2.1. Animals

Female C57BL/6J mice (4 to 5 months old) were purchased from the Guangdong Medical Laboratory Animal Center (Guangdong, China), maintained at 27°C under a reverse 12 h dark/light cycle, and food and water *ad libitum*. Experiments were approved by the committee on Animal Experimentation of Shantou University Medical College, in accordance with internationally approved regulations.

2.2. Spinal cord injury

SCI was performed as described (Mehanna et al., 2010) with 4- to 5-month-old female C57BL/6J mice. In brief, mice were anesthetized by intraperitoneal injections of ketamine (100 mg/kg, SML1873, Ketanest, Parke-Davis/Pfizer) and xylazine (5 mg/kg, X1126, Rompun, Bayer Leverkusen). A longitudinal dorsal incision was made to expose T6–T10 spinous processes. Laminectomy was performed at the T7–T9 level with mouse laminectomy forceps (Fine Science Tools, Heidelberg). The spinal cord was manually exposed, and then maximally compressed (100%) with forceps (Fine Science Tools) according to the operational definition as described (Curtis et al., 1993) for 5 s to cause a robust and reproducible lesion. Muscles and skin were then closed using 6–0 nylon stitches (Ethicon, Norderstedt, Germany). After the surgery, mice were injected intraperitoneally with 200 μl 0.9% saline solution as supplementary body

liquid. After surgery, mice were kept on a heated pad (37°C) for 8 h to prevent hypothermia and were thereafter singly housed in a temperature-controlled (26°C) room with water and soft food. During the post-operative period, the bladders were manually voided as needed.

2.3. Drug treatment

PS was dissolved in sterile PBS. Since dosages up to 60 mg/kg using intraperitoneal administration have been considered not to be toxic for rodents and since PS can cross the blood-brain-barrier, 6 and 12 mg/kg of PS were chosen as dosages (Baker et al., 1992; Paslawski et al., 1996; Musgrave et al., 2011; Chen et al., 2016). PS was administered by intraperitoneal injection once daily starting immediately following trauma until 6 weeks after SCI. PBS was administered for vehicle control. For the sham-operated controls, animals underwent a T7–T9 laminectomy without compression injury and no treatment with PS.

2.4. Assay for locomotion

The recovery of ground locomotion was evaluated by the Basso Mouse Scale (BMS) (Basso et al., 2006). In addition, we used another numerical scoring test for locomotion: single-frame motion analysis to determine the foot-stepping angle (FSA) and rump-height index (RHI) using the beam walking test (Apostolova et al., 2006; Lutz et al., 2016). The limb extension-flexion ratio (EFR) was evaluated from video from recordings of voluntary movements with the "pencil" test (Apostolova et al., 2006). Assessment was performed before and at 1, 2, 3, 4, 5 and 6 weeks after injury. Values for the left and right extremities were averaged. Recovery index (RI) was used as an estimate of functional recovery at the individual animal level as described (Pan et al., 2014). Overall RI was calculated, on an individual animal basis, as average mean values resulting from BMS score, FSA, RHI and EFR index. RI is considered as a 'clinical score' for individual mice, being based on assessment of different aspects of locomotion.

2.5. Western blot analysis of spinal cord tissue

To determine the levels of L1 protein and signal transduction molecules, spinal cords were taken to comprise an approximately 1-cm-long segment immediately proximal to the lesion site and an approximately 1.5-cm-long segment immediately distal to the lesion epicenter, 6 weeks after SCI. Tissue preparation and Western blot analysis was performed as described (Lutz et al., 2016). The following primary antibodies were used: mouse monoclonal anti-L1 antibody (1:1000, R&D Systems, MAB777); mouse monoclonal anti-extracellular signal-regulated kinases 1 and 2 (Erk1/2) antibody (1:1000, sc-135900, Santa Cruz); mouse monoclonal anti-phosphorylated Erk (p-Erk) antibody (1:1000, sc-7383, Santa Cruz); mouse monoclonal anti-protein kinase B (Akt1) antibody (1:1000, sc-55523, Santa Cruz); mouse monoclonal anti-phosphorylated Akt (p-Akt1) antibody (1:500, sc-81433, Santa Cruz); mouse monoclonal anti-B cell lymphoma 2 (Bcl-2) antibody (1:500, sc-7382, Santa Cruz); rabbit polyclonal anti-Bcl-2 associated X protein (Bax) antibody (1:1000, sc-526, Santa Cruz); rabbit polyclonal anti-mechanistic target of rapamycin (mTOR) antibody (1:1000, sc-8319, Santa Cruz); rabbit polyclonal anti-phosphorylated mTOR (p-mTOR) antibody (1:1000, sc-101738, Santa Cruz); mouse monoclonal anti-tumor protein (p53) antibody (1:1000, sc-98, Santa Cruz); mouse monoclonal anti-phosphatase and tensin homolog (PTEN) antibody (1:1000, sc-7974, Santa Cruz); rabbit polyclonal anti-casein kinase 2α (CK2α) antibody (1:1000, sc-365763, Santa Cruz), rabbit polyclonal anti-phosphorylated CK2α (p-CK2α) antibody (1:1000, 11572-1 Signalway Antibody, College Park, MD, USA); rabbit polyclonal anti-myelin basic protein (MBP) antibody (1:500, BA0094, Boster Biological Technology, Wuhan, Hubei, China); and mouse anti-monoclonal β-actin antibody (1:1000, sc-47778, Santa Cruz). Goat anti-rabbit IgG and goat anti-mouse IgG (1:1000, BA1055, BA1051, Boster) conjugated to horseradish peroxidase were used as secondary antibodies.

2.6. Immunohistology

Serial coronal sections (25 μm thick) were collected proximal and distal to lesion site at 6 weeks after SCI and processed for immunofluorescence as described (Guo & Yan, 2011). Briefly, the sections were incubated overnight at 4°C with the following primary antibodies: mouse monoclonal anti-L1 (1:200, MAB777, R&D Systems), rabbit anti-glial fibrillary acidic protein (GFAP; BA0056, 1:400, Boster) and rabbit anti-MBP (1:500, BA0094, Boster), rabbit anti-ionized calcium binding adaptor molecule (Iba-1; PB0517, 1:500, Boster), and mouse anti-neurofilament 200 (NF200; BM0100, 1:400,

Boster). The appropriate secondary antibodies were: donkey anti-mouse antibody conjugated to Dylight™ 488 (1:1000, 715-545-150, Jackson ImmunoResearch) and donkey anti-rabbit antibody conjugated to Dylight™ 568 (1:400, 711-584-152, Invitrogen, Jackson ImmunoResearch) and were incubated for 2 h at room temperature. Estimation of GFAP and Iba-1 immunoreactivities per area, numbers of L1, MBP and NF200 axons/fibers proximal and distal to lesion site was performed in double-blinded experiments as described (Mehenna et al., 2010; Sahu et al., 2018). L1 and MBP immunoreactivities were evaluated in coronal sections 4 mm proximal to lesion site, in the lesion site and 4 mm distal to lesion site (in 20 corresponding areas, 200 μm apart in consecutive sections in proximal and distal to the lesion site, and 50 μm apart in consecutive sections in lesion site) with a 40x objective. GFAP, Iba-1, and NF200 immunoreactivities were evaluated in coronal sections 4 mm proximal and 4 mm distal (in 20 corresponding areas, 200 μm apart in consecutive sections) to the lesion site. Groups consisted of 3 animals ($n = 60$ sections per group). Relative immunofluorescence intensities were measured using Image-J Pro Plus 6.0 software (Wayne Rasband, NIH).

2.7. *ELISA measurement of cytokines and biogenic amines*

For measurements of pro-inflammatory cytokine (IL-1β, IL-6 and TNF-α) and biogenic amine (5-HT and GABA) levels, spinal cord tissue was taken to comprise an approximately 1-cm-long segment immediately proximal to the lesion site and an approximately 1.5-cm-long segment immediately distal to the lesion site and including the lesion site. Tissue was taken at days 1, 7, and 14 after SCI. Analyses of pro-inflammatory cytokines and biogenic amines were performed using enzyme-linked immunosorbent assay (ELISA) kits: mouse anti-IL-1β (C701-02, GenStar), mouse anti-IL-6 (C704-02, GenStar), mouse anti-TNF-α (C708-02, GenStar), mouse anti-5-HT (MM-0443M1, MeiMian, Jiangsu, China), and mouse anti-GABA (MM-0442M2, MeiMian). All assays were carried out in triplicates following the manufacturers' instructions. Absorbance was determined using a microplate reader at 450 nm (Tecan Infinite M200 Pro, Tecan, Switzerland). The intra-assay coefficient of variation for both assays was less than 10%.

2.8. *Statistical analyses*

All statistical analyses were performed using GraphPad Prism 6 (GraphPad Software Inc., La Jolla, CA). Data are expressed as means and standard errors of the mean as indicated in the figure legends. One-way analyses of variance (ANOVA) with Tukey's *post-hoc* test were used to compare the variables among different treatment groups. Two-way ANOVA was used to analyze differences between treatment groups after SCI, and to determine changes in BMS values over time. <0.05 was considered as statistically significant.

3. Results

3.1. *Application of PS improves motor recovery after SCI*

To evaluate the effective dose of PS in SCI, we performed BMS locomotor scoring weekly up to 6 weeks with experimenter blinding on cohorts of injured mice treated with two doses of PS (6 and 12 mg/kg), or vehicle solution as a control. All mice displayed normal over-ground locomotion before injury (BMS score of 9) and a near-complete hind limb paralysis immediately after SCI (BMS score of nearly 0). From the second week onward, the hind limb locomotor functions started to improve and gradually increased week by week. Between 2 to 6 weeks after injury, the mean score values improved more in PS-treated mice than in vehicle control-treated mice. Analysis of variance (ANOVA) for repeated measurements with subsequent Tukey *post-hoc* test, both using BMS score (Fig. 1A) and BMS recovery index (Fig. 2A) revealed better recovery at 4 to 6 weeks in the PS-treated groups (6 and 12 mg/kg). In addition to the BMS, we analyzed the plantar stepping ability of the animals by measuring the foot-stepping angle (FSA). One week after injury, the FSA changed from approximately 30° before injury to 170° after injury in all groups. A decrease in FSA, which is an indicator for improved recovery, was noticed at 4 and 5 weeks after SCI in mice treated with 12 mg/kg PS, with better increases of FSA indices being observed only at 4 weeks after SCI with PS treatment after SCI (Fig. 1B, 2B). Based on these two independent measures for locomotion, our results clearly indicate that PS treatment at 12 mg/kg improves the abilities for ground locomotion after SCI.

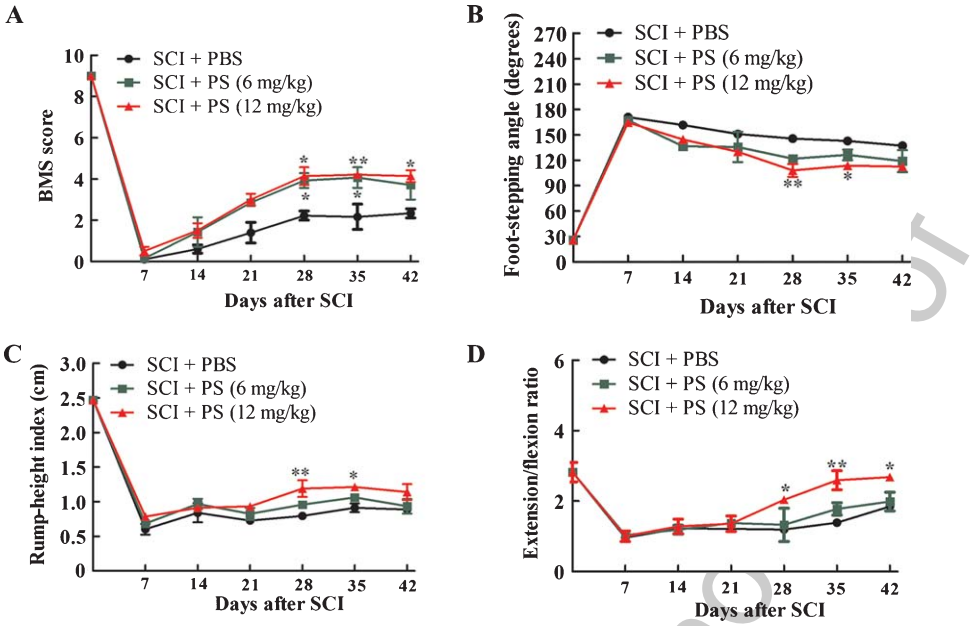

Fig. 1. Improvement of motor functions over 6 weeks after severe spinal cord compression injury of C57BL/6J female mice treated with PS. (A) BMS score, (B) foot-stepping angle (FSA), (C) rump-height index (RHI), and (D) extension/flexion ratio (EFR). ($n = 8$ mice per group; values represent means ± SEM; SCI + PBS vs. SCI + PS $^{**}p < 0.01$, $^{*}p < 0.05$, two-way ANOVA with Tukey's *post hoc* test).

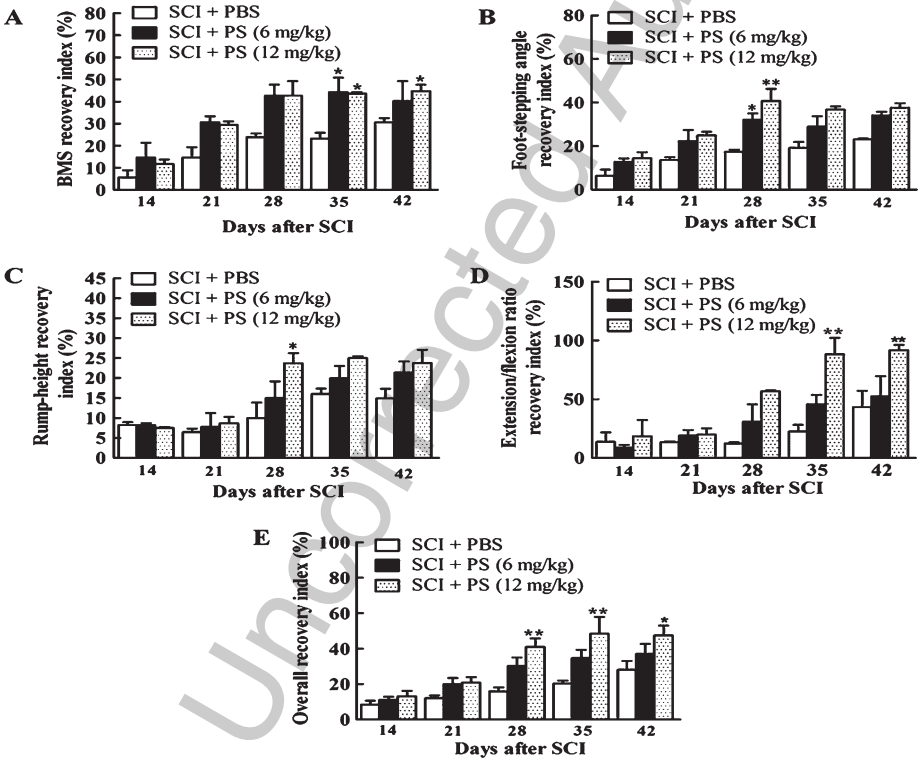

Fig. 2. Recovery indices in PS- and vehicle-treated mice after SCI. Shown are mean values ± SEM of individual recovery indices at 2 to 6 weeks after injury. (A) BMS recovery index. (B) foot-stepping angle recovery index. (C) rump-height recovery index. (D) extension/flexion ratio recovery index. (E) overall recovery index. ($n = 8$ mice per group; SCI + PBS vs. SCI + PS $^{**}p < 0.01$, $^{*}p < 0.05$, one-way ANOVA with Tukey's *post-hoc* test).

We also evaluated more complex motor functions than plantar stepping, for example the rump-height index (RHI), a measure of the ability to support body weight during ground locomotion. This ability requires coordination in different joints of both hind limb extremities, being influenced by various factors, such as stepping pattern, muscle strength, and spasticity. Analysis of the RHI also showed, in agreement with the foot-stepping angle (FSA), enhanced recovery in PS-treated mice at 12 mg/kg, but not 6 mg/kg compared to vehicle control-treated mice at 4 and 5 weeks after SCI (Fig. 1C, 2C).

The ability to perform voluntary movements without body-weight support, estimated by the extension-flexion ratio (EFR), was increased by 12 mg/kg PS treatment from week 4 onward after SCI (Fig. 1D, 2D). Finally, the overall recovery index (Fig. 2E) from individual mean values was calculated from the four different indices. The degree of overall functional improvement was higher in the 12 mg/kg PS-treated mice compared to vehicle-treated control mice at week 4 and thereafter after SCI, while the lower dose of PS (6 mg/kg) did not lead to improvement.

3.2. *PS stimulates L1 expression and proteolysis distal to the lesion site*

To evaluate the molecular consequences of PS treatment, the expression level and proteolysis of L1 were determined. To this aim, L1 protein levels in spinal cords proximal and distal to the lesion site were determined 6 weeks after SCI. Similar levels of full length L1-200 kDa and L1-70 kDa fragment were seen in the spinal cord of non-injured and sham-injured mice (Fig. 8A-C). A marked increase of full-length L1 and 70 kDa fragment levels was found distal to lesion site in mice treated with 12 mg/kg PS compared to vehicle control-treated mice (Fig. 3A-C). The levels of full-length and fragment L1 were not different from vehicle control with 6 mg/kg PS treatment and proximal to the lesion site, indicating that only a higher concentration of PS (12 mg/kg) stimulates L1 expression and proteolysis distal to the lesion site (Fig. 3 A-C). S Since MBP cleaves L1 and since this cleavage is important for myelination, we studied the generation of the L1-70 fragment after SCI (Lutz et al., 2014, 2016). Similar to L1, the level of MBP was increased distal to the lesion site with 12 mg/kg PS compared to vehicle control-treated mice (Fig. 3D, E).

We further evaluated L1 and MBP expression by immunostaining of the spinal cord following SCI in mice with and without PS treatment. L1 and MBP immunoreactivities were evaluated in coronal sections 4 mm proximal and 4 mm distal to the lesion site. A dose-dependent increase of L1 immunoreactivity was noticed distal to the lesion site with PS treatment after SCI when compared to vehicle control mice (Fig. 4A, B), whereas MBP immunoreactivity was decreased in control mice at 6 weeks after SCI. In mice treated with 12 mg/kg PS, MBP immunoreactivity was increased distal to the lesion site compared to vehicle control mice (Fig. 4C, D). SCI causes considerable myelin loss in the spinal cord distal to the lesion site, and PS treatment, especially at the 12 mg/kg dose, promotes L1 and MBP expression and remyelination and/or preserves myelinated fibers in parallel with improved functional recovery.

3.3. *PS treatment activates L1-mediated MAPK, PI3K/Akt/mTOR and CK2 signaling pathways*

In the cellular and molecular context of neurite outgrowth and neuronal survival, L1 enhances many of its beneficial functions by triggering the mitogen-activated protein kinase (MAPK), phosphoinositide 3-kinase/protein kinase B/mammalian target of rapamycin (PI3K/Akt/mTOR) and casein kinase 2 (CK2) pathways (Schmid et al., 2000; Loers et al., 2005; Maness & Schachner, 2007; Poplawski et al., 2012; Wang & Schachner, 2015).

The key component of MAPK activation, phosphorylated Erk, was determined in the spinal cord proximal and distal to lesion site. Six weeks of 12 mg/kg PS treatment leads to increases in the levels of phosphorylated Erk distal to lesion site compared to vehicle-treated control mice (Fig. 5A, B). Since the PI3K/Akt/mTOR signaling pathway has been found to be a necessary component of axonal growth, proliferation of neural stem cells and long-term potentiation, this pathway was also determined. Similar to phosphorylation of Erk, phosphorylation of mTOR and Akt was observed with 12 mg/kg PS at 6 weeks after SCI (Fig. 6A-C). The basal levels of Akt and mTOR proteins were unchanged, indicating that PS treatment triggers the phosphorylation of Akt and mTOR. We next evaluated the ability of PS to promote neuronal survival proximal and distal to the lesion site at 6 weeks after SCI. We examined the expression levels of the Bcl-2 and Bax, which regulate apoptosis. At 6 mg/kg PS treatment failed to show enhanced Bcl-2

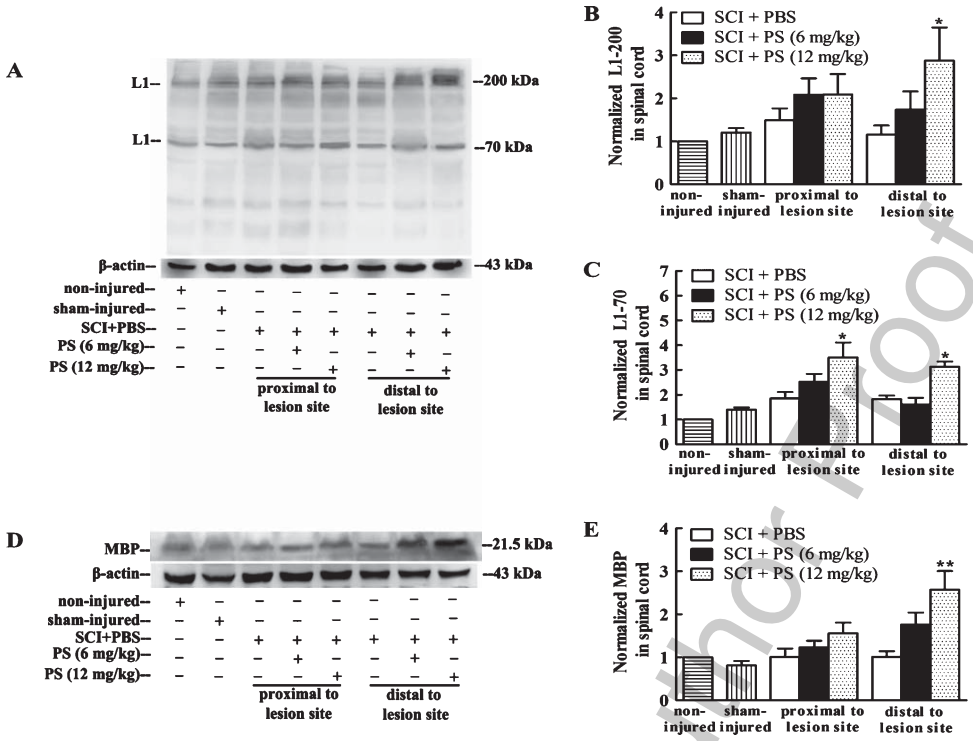

Fig. 3. PS treatment enhances L1 expression, L1 proteolysis and MBP in the spinal cord distal to lesion site 6 weeks after SCI. (A) Western blot analysis of L1 in PS- and vehicle-treated mice. (B) Normalized L1-200. (C) Normalized L1-70. (D) Western blot analysis of MBP with and without PS treatment. (E) Normalized MBP. Band densities for L1.1 and MBP were compared to β-actin levels and normalized to the non-injured control group, which was set as 1. ($n = 4$ mice per group; values represent means ± SEM; SCI vs. SCI + PS $^{**}p < 0.01$, $^{*}p < 0.05$, one-way ANOVA, Tukey's *post-hoc* test).

levels proximal and distal to lesion site, whereas PS treatment at 12 mg/kg increased Bcl-2 levels proximal to lesion site (Fig. 6A, D). The level of Bax was increased in the spinal cord of injured mice compared to uninjured mice at 6 weeks after SCI. Daily PS treatment for six weeks following SCI led to decrease in the levels of Bax in proximal and distal to lesion site but failed to reach significant levels (Fig. 6A, E).

To link PS-mediated L1 activation to CK2α, PTEN and p53 functions, we determined phosphorylated CK2α, CK2α protein, and the tumor suppressors PTEN and p53 at 6 weeks after SCI distal to the lesion site. Both concentrations of PS stimulated the phosphorylation of CK2α, with higher phosphorylation being seen with the 12 mg/kg dose compared to vehicle control-treated mice (Fig. 7A, B). Levels of PTEN and p53 were increased at 6 weeks after SCI, when compared to sham-injured and non-injured groups. PS treatment at 12 mg/kg decreased PTEN levels in the spinal cord distal to lesion site at 6 weeks after SCI (Fig. 7A, C). Dose-dependent decreases of the levels of p53 were observed proximally and distally to lesion site, and a higher inhibition was noticed distal to lesion site at 12 mg/kg dose compared to vehicle control-treated mice (Fig. 7A, D). These data indicate that PS triggers beneficial L1 functions by inhibiting PTEN and p53 in parallel with activating CK2α.

3.4. PS treatment reduces astrogliosis, decreases the microglial/macrophage response, and promotes the levels of neurofilament

Immunohistochemical analysis was used to further document the impact of PS treatment on molecular hallmarks of astrogliosis commonly seen after SCI, by measuring expression of GFAP, a marker for astrocytes (Biber et al., 2007). At 6 weeks after injury, PS-treated mice (12 mg/kg) showed less intense astrogliosis caudal and distal to lesion site compared to vehicle control-treated mice (Fig. 8A, B), similar to observations on astrogliosis correlating negatively with locomotor activity as measured by BMS (Jakovcevski et al., 2007; Lee et al., 2012; Wu et al., 2012). Since microglia/macrophage responses

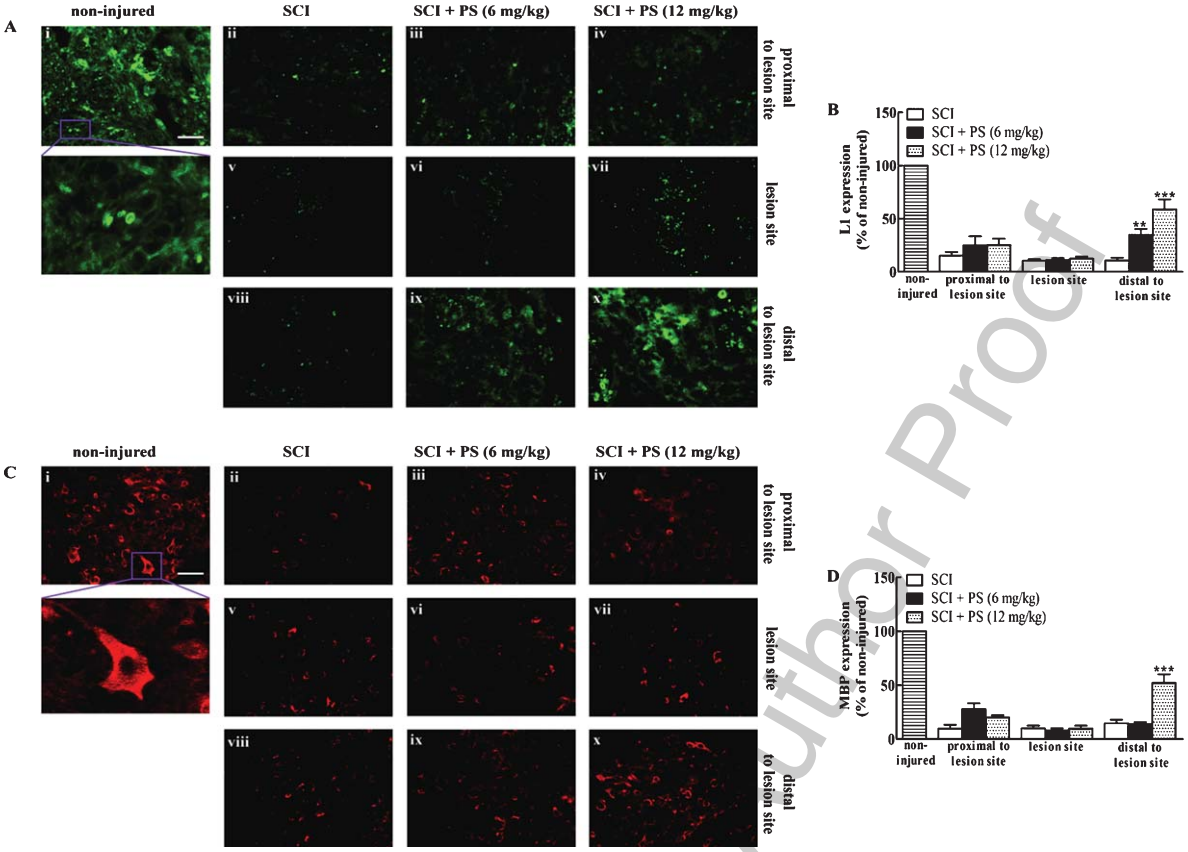

Fig. 4. Immunohistochemical analysis of L1 and MBP expression 6 weeks after SCI, caudal and distal to lesion site. (A) Representative images of coronal sections stained with antibodies against L1. Scale bar, 50 μm for all images. (B) Quantification of L1-immunoreactivity. (C) Representative images of coronal sections stained with antibodies against MBP. Scale bar, 50 μm for all images. (D) Quantification of L1-immunoreactivity. Quantification was performed in coronal sections 4 mm proximal and 4 mm distal to the lesion site (in 20 corresponding sections, consecutive sections 200 μm apart proximal and distal to lesion site, and 50μm apart in the lesion site. Groups consisted of 3 animals, $n = 60$ sections per group). Photomicrographs were taken from the dorsal column white matter. i) Non-injured spinal cord. Spinal cord proximal to the lesion site: ii) SCI + PBS, iii) SCI + PS (6 mg/kg), iv) SCI + PS with (12 mg/kg). Lesion site: v) SCI + PBS, vi) SCI + PS (6 mg/kg), vii), SCI + PS (12 mg/kg). Spinal cord distal to lesion site: viii) SCI + PBS, ix) SCI + PS (6 mg/kg), x) SCI + PS with (12 mg/kg). Rectangle shows the magnified area with L1 and MBP immunopositivities (Values represent means ± SEM; SCI + PBS vs. SCI + PS $^{***}p < 0.001$, $^{**}p < 0.01$, $^{*}p < 0.05$, one-way ANOVA with Tukey's *post-hoc* test).

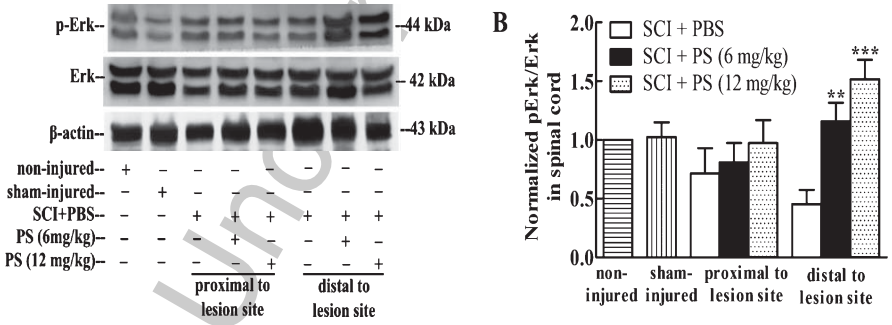

Fig. 5. PS treatment activates the MAPK signaling pathway after SCI. (A) Western blot analysis of p-Erk and Erk 6 weeks after SCI in vehicle- and PS-treated mice. (B) Normalized p-Erk/Erk. Band intensities for p-Erk/Erk were compared to β-actin levels and normalized to the non-injured control group, which was set as 1. ($n = 4$ mice per group; values represent means ± SEM; SCI + PBS vs. SCI + PS $^{*}p < 0.05$, one-way ANOVA with Tukey's *post-hoc* test).

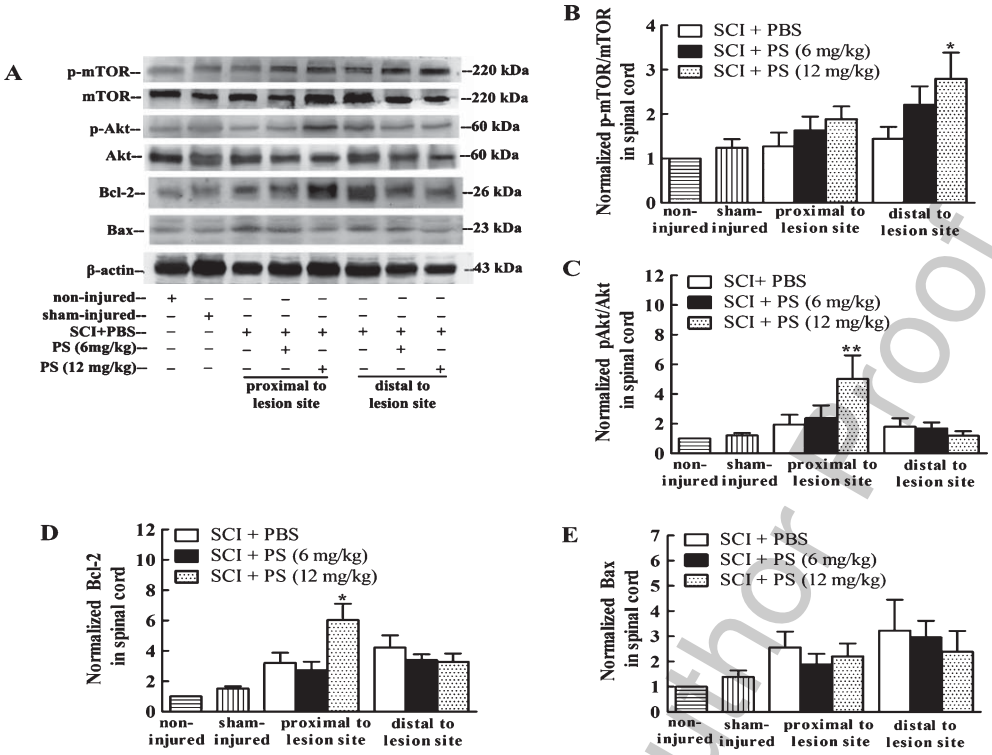

Fig. 6. PS treatment stimulates the PI3/AKT/mTOR signaling pathway after SCI. (A) Western blot analysis of p-mTOR, mTOR, p-AKT, AKT, Bcl-2 and Bax 6 weeks after SCI with PBS or PS treatment. (B) Normalized p-mTOR/mTOR. (C) Normalized p-AKT/AKT. (D) Normalized Bcl-2. (E) Normalized Bax. Signal intensities of β-actin were used for normalization ($n = 4$ mice per group; values represent means ± SEM; SCI + PBS vs. SCI + PS $^{**}p < 0.01$, $^{*}p < 0.05$, one-way ANOVA with Tukey's *post-hoc* test).

play an important role in regeneration (Streit et al., 1999; Wu et al., 2012), immunoreactive Iba-1 cells were determined by Image-J quantification of fluorescence intensity in coronal sections both proximal and distal to lesion site. A decrease of Iba-1 immunoreactivity was observed with PS treatment (12 mg/kg) at 6 weeks after injury (Fig. 8C, D). Thus, PS treatment decreases the microglial/macrophage response in the vicinity of the lesion site.

Six weeks after injury, neurofilament 200 (NF-200) immunoreactive cell bodies were seen in all groups - with nerve fibers discernible in coronal sections. NF-200 immunoreactivity was increased both proximal and distal to the lesion site at 12 mg/kg compared to vehicle control-treated mice (Fig. 8E, F), indicating protection of neurons.

3.5. *PS treatment reduces inflammatory cytokine levels during the acute stage of inflammation after SCI*

The pro-inflammatory cytokines interleukin (IL)-1β, IL-6, and tumor necrosis factor-α (TNF-α) play important roles in secondary injury following SCI (Rock et al., 2004). We therefore evaluated the influence of PS on inflammation by measuring the levels of pro-inflammatory markers IL-1β, IL-6 and TNF-α in the spinal cord at days 1, 7 and 14 after SCI. All cytokines were elevated in the acute phase of inflammation after injury in vehicle-treated mice (Fig. 9A-C). PS treatment reduced cytokine levels at days 1 and 7 after SCI (Fig. 9A-C). With PS treatment, the decrease of IL-1β and TNF-α levels was more profound than that of IL-6 levels (Fig. 9A-C). No difference of cytokine levels between groups was detected in the chronic phase of inflammation (day 14). These data indicate that PS exerts an anti-inflammatory role in the acute stage of SCI.

We also examined levels of 5-HT and GABA and found that PS-treated mice showed higher levels of 5-HT and GABA in the lesion site at days 1, 7 and 14 after SCI compared to non-injured and vehicle control-treated mice (Fig. 9D, E). These observations indicate that PS beneficially influences the levels of these compounds.

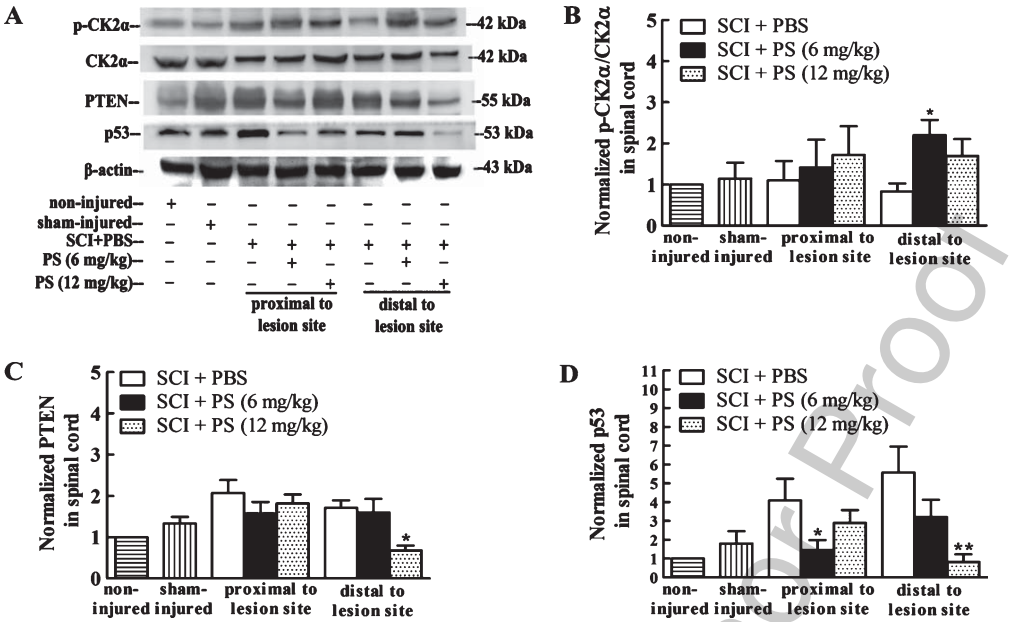

Fig. 7. PS treatment activates the CK2 signaling pathway after SCI. (A) Western blot analysis of p-CK2α, CK2α, PTEN and p53 after SCI with or without PS treatment. (B) Normalized p-CK2α/CK2α. (C) Normalized PTEN. (D) Normalized p53. ($n = 4$ mice per group; values represent means ± SEM; SCI vs. SCI + PS $^{**}p < 0.01$, $^{*}p < 0.05$, one-way ANOVA with Tukey's *post-hoc* test).

4. Discussion

Based on the success of using the small organic L1 mimetic compound PS as an enhancer of neurite outgrowth, neuronal survival, Schwann cell migration, proliferation and myelination *in vitro* (Kataria et al., 2016), we have continued to study the effect of PS in a mouse model of SCI. The enhanced overall motor performance of PS-treated mice at 4 weeks after lesioning was observed by 4 different parameters: BMS, FSA, RHI, and EFR. This improvement correlates with increases in L1 levels which is noteworthy, since PS interacts with the function triggering epitope in the third fibronectin type III homologous domain of L1 (Kataria et al., 2016). This epitope had been shown not only to trigger the beneficial functions of L1, also to enhance L1 expression. We here also observed that PS treatment not only enhanced levels of full-length L1 but also of the proteolytic 70 kDa fragment proximal and distal to lesion site. L1 fragments have been shown to be important for neurite outgrowth, neuronal migration, neuronal survival and myelination, as demonstrated in vitro (Lutz et al., 2014) and *in vivo* (Lutz et al., 2016; Kataria et al., 2016; Sahu et al., 2018). In the present study, up-regulation of L1 expression likely contributes to the success in functional recovery. Furthermore, PS reduced astrogliosis and microglial activation at the lesion site, thus also probably contributing to benefits in recovery. Like L1, PS up-regulates MBP expression and promotes myelinogenesis by inducing differentiation of oligodendrocyte progenitor cells after SCI (Barbin et al., 2004; Chen et al., 2007). These observations are in agreement with the findings on improved remyelination after L1 overexpression in the lesioned mouse peripheral nervous system (Guseva et al., 2011) and beneficial effects of the L1 mimetic small organic molecules duloxetine and piceid after injury (Kataria et al., 2016). PS was reported to bind to the third fibronectin type III domain of L1, thereby stimulating *in vitro* L1-mediated functions, such as neurite outgrowth, neuronal migration, Schwann cell migration, proliferation and myelination, similar to L1-Fc (Kataria et al., 2016).

Since PS/L1 interactions lead to enhanced phosphorylation of Erk, Akt, mTOR and CK2 via MAPK, PI3K/Akt/mTOR and CK2α signaling pathways, as shown in the present study, we infer that PS-mediated enhanced phosphorylation underlies axonal regrowth/sparing and functional recovery after SCI. PS treatment also enhances p-Akt and Bcl-2 expression, indicating a neuroprotective role of PS after trauma. We now also show that PS-induced neuroprotection can be attributed to the ability of PS to inhibit inflammation as described (Benson et al., 2013; Cebak et al., 2017). In addition, PS, as a potent

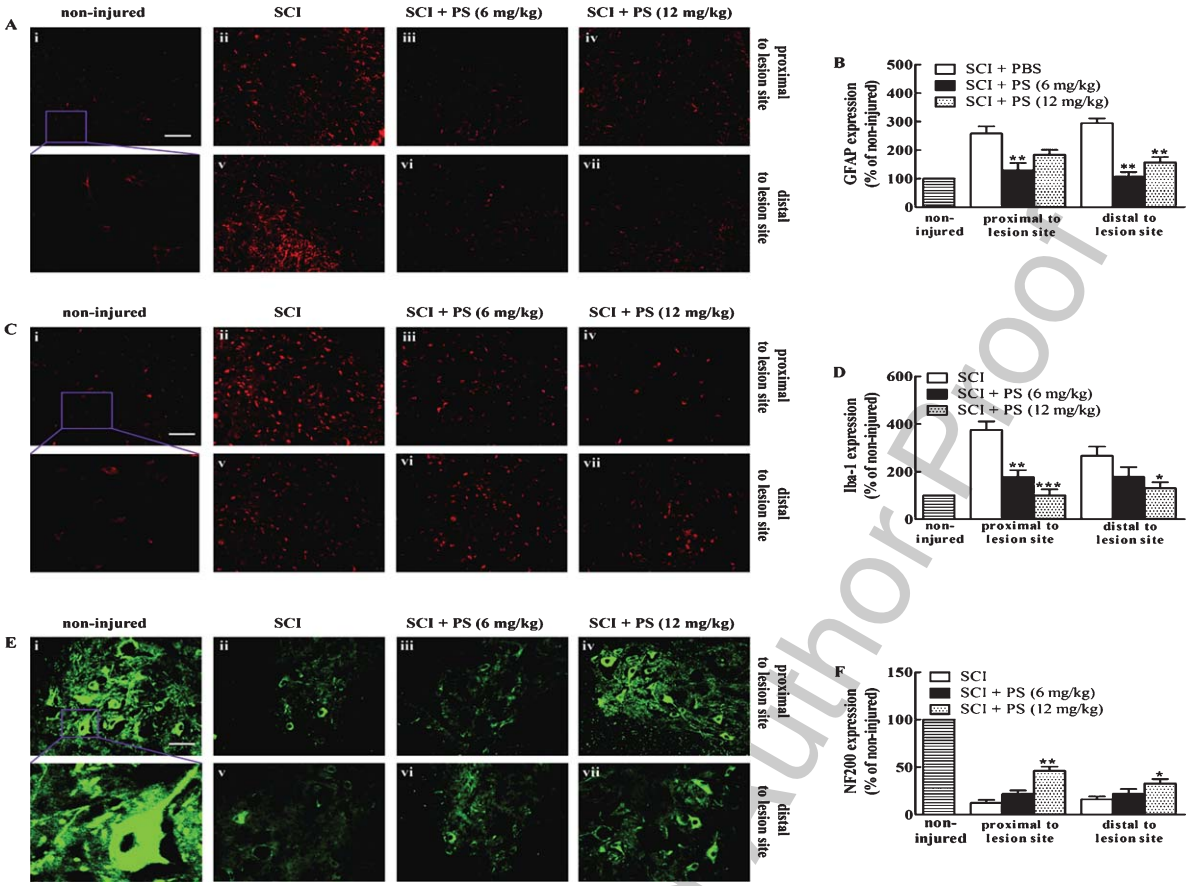

Fig. 8. PS treatment reduces astrogliosis, attenuates activation of microglia/macrophages, and enhances regrowth of axons 6 weeks after SCI. (A) Representative images of coronal sections stained with antibodies against GFAP. (B) Quantification of GFAP-immunoreactivity. (C) Representative images of coronal sections stained with antibodies against Iba-1. (D) Quantification of Iba-1^{+}-immunoreactivity. (E) Representative images of coronal sections stained with antibodies against NF-200. (F) Quantification of NF-200^{+}-immunoreactivity. Quantification of GFAP, Iba-1^{+} and NF-200^{+} immunoreactivities were evaluated in coronal sections 4 mm proximal and 4 mm distal to the lesion site (in 20 corresponding sections, consecutive sections 200 μm apart. Groups consisted of 3 animals, $n = 60$ sections per group). Photomicrographs were taken from the dorsal column white matter. i) Non-injured spinal cord. Spinal cord proximal to lesion site: ii) SCI + PBS, iii) SCI + PS (6 mg/kg), iv) SCI + PS with (12 mg/kg). Spinal cord distal to the lesion site: v) SCI + PBS, vi) SCI + PS (6 mg/kg), vii) SCI + PS with (12 mg/kg). Rectangle shows the magnified area with GFAP, Iba-1, and NF200 immunoreactivities. (Scale bar, 50 μm, for all images. Values represent means ± SEM; SCI + PBS vs. SCI + PS $^{***}p < 0.001$, $^{**}p < 0.01$, $^{*}p < 0.05$, one-way ANOVA with Tukey's *post-hoc* test).

monoamine oxidase inhibitor, increases basal 5-HT levels at the lesion site. Monoaminergic neurotransmission, and, in particular 5-HT, is important for initiation and modulation of locomotor patterns during walking (Barbeau & Rossignol, 1991) and ventral spinal cord 5-HT innervation correlates with motor activity (Pearse et al., 2004; Fouad et al., 2005), with ventral horn 5-HT being linked to locomotor function, and 5-HT improving locomotion after SCI (Zhou & Goshgarian, 2000; Hayashi et al., 2010). Interestingly, the acrolein scavenging properties of PS mitigate sensory and motor deficits after SCI (Chen et al., 2016). Moreover, acute and chronic treatments with PS reduce depolarization-induced outflow of the excitatory neurotransmitter glutamate (Michael-Titus et al., 2000). The combined observations indicate that PS-induced functional recovery is multifactorial.

Beneficial L1 functions in several injury models (Irintchev & Schachner, 2012) are now reproduced by PS, which decreases pro-inflammatory cytokine levels (IL-1β, TNF-α, IL-6) in the acute phase after SCI, most likely contributing via its anti-inflammatory activities to recovery after SCI. Notably, down-regulation of neuronal L1 expression is an adaptive process of neuronal

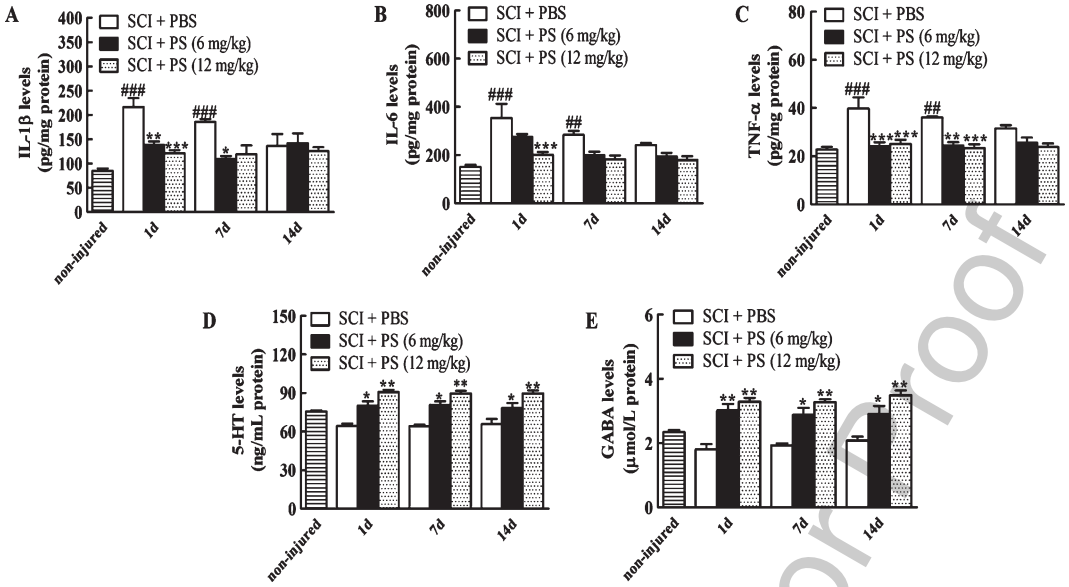

Fig. 9. PS treatment reduces pro-inflammatory cytokine levels and increases of biogenic amine levels at 6 weeks after SCI. Levels of pro-inflammatory cytokines (IL-1β, IL-6 and TNF-α) and biogenic amines (5-HT and GABA) were determined by ELISA in homogenates from non-injured and injured spinal cord obtained at days 1, 7 and 14 after application of PS (6 and 12 mg/kg) and PBS vehicle control. Levels of (A) IL-1β, (B) IL-6, (C) TNF-α, (D) 5-HT, (E) GABA. Four mice were analyzed per group, and the experiment was performed independently 3 times. (Values represent means ± SEM; SCI + PBS vs. SCI + PS $^{***}p < 0.001$, $^{**}p < 0.01$, $^{*}p < 0.05$; non-injured vs. SCI+PBS $^{###}p < 0.001$, $^{##}p < 0.01$, one-way ANOVA with Tukey's *post-hoc* test).

self-defense in response to pro-inflammatory T-cells, thereby alleviating immune-mediated axonal injury in experimental autoimmune encephalomyelitis (Menzel et al., 2016). Increased levels of monoamines, especially 5-HT as well as of GABA by PS treatment likely also contribute toward anti-inflammatory functions. In agreement, 5-HT and GABA reduce the severity of experimental autoimmune encephalomyelitis through anti-inflammatory mechanisms (Hofstetter et al., 2005; Levite, 2008; Bhat et al., 2010; Benson et al., 2013). Sustained presence of 5-HT and GABA interacting with T-cells and macrophages modulate the proliferation of the T-cells and cytokine release (Yin et al., 2006; Bhat et al., 2010; Mendu et al., 2012). In addition, PS modulates immune functions by inhibiting MAO-A, which is expressed in mitochondria of lymphocytes (Yin et al., 2006). The PS metabolite β-phenylethylidene hydrazine, a potent inhibitor GABA transaminase, increases GABA levels in the immune system (Benson et al., 2013). Vigabatrin and gabaculin, irreversible inhibitors of GABA transaminase, reduce IL-1 and IL-6 expression in macrophages (Bhat et al., 2010). Together with these reports, our results support the idea that PS is beneficial through reducing information in the acute phase after SCI. Moreover, PS application reduces the depolarization-induced outflow of excitatory glutamate (Michael-Titus et al., 2000).

Based our study, we propose that PS increases neuroprotection and recovery after spinal cord injury via multiple mechanisms: PS, as a L1 mimetic, stimulates L1 expression and its functions thus promoting functional recovery, axonal regeneration/sparing, and remyelination. In addition, we propose that reducing inflammation also contributes to enhancing repair. We conclude that our study provides novel insights into the role of PS in L1-mediated beneficial functions. With PS being able to penetrate the blood brain barrier, this FDA-approved drug encourages hopes for clinical application.

ACKNOWLEDGMENTS

We are very grateful to Professor Junhui Bian, Dean of Shantou University Medical College, and Dr. Frieda Law, advisor to the Li Kashing Foundation, for support. We thank Dr. Stanley Li Lin for some editing. This work was funded by the Li Kashing Foundation.

References

Apostolova, I., Irintchev, A., & Schachner, M. (2006). Tenascin-R restricts posttraumatic remodeling of motoneuron innervation and functional recovery after spinal cord injury in adult mice. *Journal of Neuroscience*, *26*, 7849-7859.

Baker, G.B., Coutts, R.T., McKenna, K.F., & Sherry-McKenna, R.L. (1992). Insights into the mechanisms of action of the MAO inhibitors phenelzine and tranylcypromine: A review. *Journal of Psychiatry & Neuroscience*, *17*, 206-214.

Barbeau. H., & Rossignol, S. (1991). Initiation and modulation of the locomotor pattern in the adult chronic spinal cat by noradrenergic, serotonergic and dopaminergic drugs. *Brain Research*, *546*, 250-260.

Barbin, G., Aigrot, M.S., Charles, P., Foucher, A., Grumet, M., Schachner, M., Zalc, B., & Lubetzki, C. (2004). Axonal cell-adhesion molecule L1 in CNS myelination. *Neuron Glia Biology*, *1*, 65-72.

Basso, D.M., Fisher, L.C., Anderson, A.J., Jakeman, L.B., McTigne, D.M., & Popovich, P.G. (2006). Basso mouse scale for locomotion defects differentiation in recovery after spinal cord injury in five common mouse strains. *Journal of Neurotrauma*, *23*, 635-659.

Benson, C.A., Wong, G., Tenorio, G., Baker, G.B., & Kerr, B.J. (2013). The MAO inhibitor phenelzine can improve functional outcomes in mice with established clinical signs in experimental autoimmune encephalomyelitis (EAE). *Behavioral Brain Research*, *252*, 302-311.

Bhat, R., Axtell, R., Mitra, A., Miranda, M., Lock, C., Tsien, R.W., & Steinman, L. (2010). Inhibitory role for GABA in autoimmune inflammation. *Proceedings of the National Academy of Sciences of the United States of America*, *107*, 2580-2585.

Biber, K., Neumann, H., Inoue, K., & Boddeke, H.W. (2007). Neuronal 'on' and 'off' signals control microglia. *Trends in Neuroscience*, *30*, 596-602.

Cebak, J.E., Singh, I.N., Hill, R.L., Wang, J.A., & Hall, E.D. (2017). Phenelzine protects brain mitochondrial function *in vitro* and *in vivo* following traumatic brain injury by scavenging the reactive carbonyls 4-hydroxynonenal and acrolein leading to cortical histological neuroprotection. *Journal of Neurotrauma*, *34*, 1302-1317.

Chaitidis, P., Billett, E.E., O'Donnell, V.B., Fajardo, A.B., Fitzgerald, J., Kuban, R.J., Ungethuem, U., & Kühn, H. (2004). Th2 response of human peripheral monocytes involves isoform-specific induction of monoamine oxidase-A. *Journal of Immunology*, *173*, 4821-4827.

Chen, J., Wu, J., Apostolova, I., Skup, M., Irintchev, A., Kügler, S., & Schachner, M. (2007). Adeno-associated virus-mediated L1 expression promotes functional recovery after spinal cord injury. *Brain*, *130*, 954-969.

Chen, Z., Park, J., Butler, B., Acosta, G., Vega-Alvarez, S., Zheng, L., Tang, J., McCain, R., Zhang, W., Ouyang, Z., Cao, P., & Shi, R. (2016). Mitigation of sensory and motor deficits by acrolein scavenger phenelzine in a rat model of spinal cord contusive injury. *Journal of Neurochemistry*, *138*, 328-338.

Curtis, R., Green, D., Lindsay, R.M., & Wilkin, G.P. (1993). Up-regulation of GAP-43 and growth of axons in rat spinal cord after compression injury. *Journal of Neurocytology*, *22*, 51-64.

Dong, L., Chen, S., & Schachner, M. (2003). Single chain Fv antibodies against neural cell adhesion molecule L1 trigger L1 functions in cultured neurons. *Molecular Cell Neuroscience*, *22*, 234-247.

Fehlings, M.G. (2008). Repair of the chronically injured human spinal cord. *Journal of Neurosurgery: Spine*, *8*, 205-207.

Fitch, M.T., & Silver, J. (2008). CNS injury, glial scars, and inflammation: Inhibitory extracellular matrices and regeneration failure. *Experimental Neurology*, *209*, 294-301.

Fouad, K., Schnell, L., Bunge, M.B., Schwab, M.E., Liebscher, T., & Pearse, D.D. (2005). Combining Schwann cell bridges and olfactory-ensheathing glia grafts with chondroitinase promotes locomotor recovery after complete transection of the spinal cord. *Journal of Neuroscience*, *25*, 1169-1178.

Giger, R.J., Hollis, E.R., & Tuszynski, M.H. (2010). Guidance molecules in axon regeneration. *Cold Spring Harbor Perspectives in Medicine*, *2*, a001867.

Guseva, D., Zerwas, M., Xiao, M.F., Jakovcevski, I., Irintchev, A., & Schachner, M. (2011). Adhesion molecule L1 overexpressed under the control of the neuronal Thy-1 promoter improves myelination after peripheral nerve injury in adult mice. *Experimental Neurology*, *229*, 339-352.

Guo, Y., & Yan, K.P. (2011). Prognostic significance of urine neutrophil gelatinase-associated lipocalin in patients with septic acute kidney injury. *Experimental & Therapeutic Medicine*, *2*, 1133-1139.

Hayashi, Y., Jacob-Vadakot, S., Dugan, E.A., McBride, S., Olexa, R., Simansky, K., Murray, M., & Shumsky, J.S. (2010). 5-HT precursor loading: But not 5-HT receptor agonists, increases motor function after spinal cord contusion in adult rats. *Experimental Neurology*, *221*, 68-78.

Hofstetter, H.H., Mossner, R., Lesch, K.P., Linker, R.A., Toyka, K.V., & Gold, R. (2005). Absence of reuptake of serotonin influences susceptibility to clinical autoimmune disease and neuroantigen-specific interferon-gamma production in mouse EAE. *Clinical Experimental Immunology*, *142*, 39-44.

Huang, W.C., Yang, C.C., Chen, I.H., Liu, Y.M., Chang, S.J., & Chuang, Y.J. (2013). Treatment of glucocorticoids inhibited early immune responses and impaired cardiac repair in adult zebrafish. *PLoS One*, *8*, e66613.

Irintchev, A., & Schachner, M. (2012). The injured and regenerating nervous system: Immunoglobulin superfamily members as key players. *Neuroscientist*, *18*, 452-466.

Jakovcevski, I., Wu, J., Karl, N., Leshchyns'ka, I., Sytnyk, V., Chen, J., Irintchev, A., & Schachner, M. (2007). Glial scar expression of CHL1, the close homolog of the adhesion molecule L1, limits recovery after spinal cord injury. *Journal of Neuroscience*, *27*, 7222-7233.

Johnson, M.R., Lydiard, R.B., & Ballenger, J.C. (1995). Panic disorder Pathophysiology and drug treatment. *Drugs*, *49*, 328-334.

Kataria, H., Lutz, D., Chaudhary, H., Schachner, M., & Loers, G. (2016). Small molecule agonists of cell adhesion molecule L1 mimic L1 functions *in vivo*. *Molecular Neurobiology*, *53*, 4461-4483.

Lavdas, A.A., Papastefanaki, F., Thomaidou, D., & Matsas, R. (2011). Cell adhesion molecules in gene and cell therapy approaches for nervous system repair. *Current Gene Therapy*, *11*, 90-100.

Lee, H.J., Bian, S., Jakovcevski, I., Wu, B., Irintchev, A., & Schachner, M. (2012). Delayed applications of L1 and chondroitinase ABC promote recovery after spinal cord injury. *Journal of Neurotrauma*, *29*, 1850-1863.

Levesque, M., Feng, Y., Jones, R.A., & Martin, P. (2013). Inflammation drives wound hyperpigmentation in zebrafish by recruiting pigment cells to sites of tissue damage. *Disease Models & Mechanisms*, *6*, 508-515.

Levite, M. (2008). Neurotransmitters activate T-cells and elicit crucial functions via neurotransmitter receptors. *Current Opinion in Pharmacology*, *8*, 460-471.

Loers, G., Chen, S., Grumet, M., & Schachner, M. (2005). Signal transduction pathways implicated in neural recognition molecule L1 triggered neuroprotection and neuritogenesis. *Journal of Neurochemistry*, *92*, 1463-1476.

Lutz, D., Loers, G., Kleene, R., Oezen, I., Kataria, H., Katagihallimath, N., Braren, I., Harauz, G., & Schachner, M. (2014). Myelin basic protein cleaves cell adhesion molecule L1 and promotes neuritogenesis and cell survival. *Journal of Biological Chemistry*, *289*, 13503-13518.

Lutz, D., Kataria, H., Kleene, R., Loers, G., Chaudhary, H., Guseva, D., Wu, B., Jakovcevski, I., & Schachner, M. (2016). Myelin basic protein cleaves cell adhesion molecule L1 and improves regeneration after injury. *Molecular Neurobiology*, *53*, 3360-3376.

Maness, P.F., & Schachner, M. (2007). Neural recognition molecules of the immunoglobulin superfamily: Signaling transducers of axon guidance and neuronal migration. *Nature Neuroscience*, *10*, 19-26.

Mehanna, A., Mishra, B., Kurschat, N., Schulze, C., Bian, S., Loers, G., Irintchev, A., & Schachner, M. (2009). Polysialic acid glycomimetics promote myelination and functional recovery after peripheral nerve injury in mice. *Brain*, *132*, 1449-1462.

Mehanna, A., Jakorcevski, I., Acar, A., Xiao, M., Loers, G., Rougon, G., Irintchev, A., & Schachner, M. (2010). Polysialic acid glycomimetic promotes functional recovery and plasticity after spinal cord injury in mice. *Molecular Therapeutics*, *18*, 34-43.

Mendu, S.K., Bhandage, A., Jin, Z., & Birnir, B. (2012). Different subtypes of GABA-A receptors are expressed in human, mouse and rat T lymphocytes. *PLoS One*, *7*, e42959.

Menzel, L., Paterka, M., Bittner, S., White, R., Bobkiewicz, W., van Horssen, J., Schachner, M., Witsch, E., Kuhlmann, T., Zipp, F., & Schafer, M.K. (2016). Down-regulation of neuronal L1 cell adhesion molecule expression alleviates inflammatory neuronal injury. *Acta Neuropathologica*, *132*, 703-720.

Michael-Titus, A.T., Bains, S., Jeetle, J., & Whelpton, R. (2000). Imipramine and phenelzine decrease glutamate overflow in the prefrontal cortex-a possible mechanism of neuroprotection in major depression? *Neuroscience*, *100*, 681-684.

Musgrave, T., Benson, C., Wong, G., Browne, I., Tenorio, G., Rauw, G., Baker, G.B., & Kerr, B.J. (2011). The MAO inhibitor phenelzine improves functional outcomes in mice with experimental autoimmune encephalomyelitis (EAE). *Brain Behavior & Immunity*, *25*, 1677-1688.

Pan, H.C., Shen, Y.Q., Loers, G., Jakovcevski, I., & Schachner, M. (2014). Tegaserod, a small compound mimetic of polysialic acid, promotes functional recovery after spinal cord injury in mice. *Neuroscience*, *26*, 356-366.

Parent, M.B., Master, S., Kashlub, S., & Baker, G.B. (2002). Effects of the antidepressant/antipanic drug phenelzine and its putative metabolite phenylethylidenehydrazine on extracellular gamma-aminobutyric acid levels in the striatum. *Biochemical Pharmacology*, *63*, 57-64.

Paslawski, T., Treit, D., Baker, G.B., George, M., & Coutts, R.T. (1996). The antidepressant drug phenelzine produces antianxiety effects in the plus-maze and increases in rat brain GABA. *Psychopharmacology*, *127*, 19-24.

Paslawski, T., Knause, E., Iqbal, N., Coutts, R.T., & Baker, G.B. (2001). Beta-phenylethylidenehydrazine, a novel inhibitor of GABA transaminase. *Drug Development Research*, *54*, 35-39.

Pearse, D.D., Pereira, F.C., Marcillo, A.E., Bates, M.L., Berrocal, Y.A., Filbin, M.T., & Bunge, M.B. (2004). cAMP and Schwann cells promote axonal growth and functional recovery after spinal cord injury. *Nature Medicine*, *10*, 610-616.

Poplawski, G.H., Tranziska, A.K., Leshchyns'ka, I., Meier, I.D., Streichert, T., Sytnyk, V., & Schachner, M. (2012). L1CAM increases MAP2 expression via the MAPK pathway to promote neurite outgrowth. *Molecular Cellular Neuroscience*, *50*, 169-178.

Rock, R.B., Gekker, G., Hu, S., Sheng, W. S., Cheeran, M., Lokensgard, J.R. & Peterson, P.K. (2004). Role of microglia in central nervous system infections. *Clinical Microbiology Reviews*, *17*, 942-964.

Sahu, S., Zhang, Z., Li, R., Hu, J.K., Shen, H.F., Loers, G., Shen, Y., & Schachner, M. (2018). Small organic compound mimicking the L1 cell adhesion molecule promotes functional recovery after spinal cord injury in zebrafish. *Molecular Neurobiology*, *55*, 859-878.

Schmid, R.S., Pruitt, W.M., & Maness, P.F. (2000). A MAP kinase-signaling pathway mediates neurite outgrowth on L1 and requires Src-dependent endocytosis. *Journal of Neuroscience*, *20*, 4177-4188.

Simonini, M.V., Polak, P.E., Sharp, A., McGuire, S., Galea, E., & Feinstein, D.L. (2010). Increasing CNS noradrenaline reduces EAE severity. *Journal of Neuroimmune Pharmcology*, *5*, 252-259.

Singh, I.N., Gilmer, L.K., Miller, D.M., Cebak, J.E., Wang, J.A., & Hall, E.D. (2013). Phenelzine mitochondrial functional preservation and neuroprotection after traumatic brain injury related to scavenging of the lipid peroxidation-derived aldehyde 4-hydroxy-2-nonenal. *Journal of Cerebral Blood Flow Metabolism*, *33*, 593-599.

Streit, W.J., Walter, S.A., & Pennell, N.A. (1999). Reactive microgliosis. *Progress in Neurobiology*, *57*, 563-581.

Sytnyk, V., Leshchyns'ka, I., & Schachner, M. (2017). Neural cell adhesion molecules of the immunoglobulin superfamily regulate synapse formation, maintenance and function. *Trends in Neuroscience*, *40*, 295-308.

Wang, Y., & Schachner, M. (2015). The intracellular domain of L1CAM binds to casein kinase 2α and is neuroprotective via inhibition of the tumor suppressors PTEN and p53. *Journal of Neurochemistry*, *133*, 828-843.

Wu, B., Matic, D., Djogo, N., Szpotowicz, E., Schachner, M., & Jakovcevski, I. (2012). Improved regeneration after spinal cord injury in mice lacking functional T- and B-lymphocytes. *Experimental Neurology*, *237*, 274-285.

Yin, J., Albert, R.H., Tretiakova, A.P., & Jameson, B.A. (2006). 5-HT(1B) receptors play a prominent role in the proliferation of T-lymphocytes. *Journal of Neuroimmunology*, *181*, 68-81.

Yoo, M., Khaled, M., Gibbs, K.M., Kim, J., Kowalewski, B., Dierks, T., & Schachner, M. (2013). Arylsulfatase B improves locomotor function after mouse spinal cord injury. *PLoS One*, *8*, e57415.

Zhou, S.Y., & Goshgarian, H.G. (2000). 5-Hydroxytryptophan-induced respiratory recovery after cervical spinal cord hemisection in rats. *Journal of Applied Physiology*, *89*, 1528-1536.